Molecular Biology of the Cell
Vol. 17, 336–344, January 2006

CAR-1, a Protein That Localizes with the mRNA Decapping Component DCAP-1, Is Required for Cytokinesis and ER Organization in *Caenorhabditis elegans* Embryos[D] [V]

Jayne M. Squirrell,* Zachary T. Eggers,* Nancy Luedke,* Bonnie Saari,† Andrew Grimson,† Gary E. Lyons,‡ Philip Anderson,† and John G. White*‡

*Laboratory for Molecular Biology and Departments of †Genetics and ‡Anatomy, University of Wisconsin, Madison, WI 53706

Submitted September 20, 2005; Accepted October 20, 2005
Monitoring Editor: Martin Chalfie

The division of one cell into two requires the coordination of multiple components. We describe a gene, *car-1*, whose product may provide a link between disparate cellular processes. Inhibition of *car-1* expression in *Caenorhabditis elegans* embryos causes late cytokinesis failures: cleavage furrows ingress but subsequently regress and the spindle midzone fails to form, even though midzone components are present. The localized accumulation of membrane that normally develops at the apex of the cleavage furrow during the final phase of cytokinesis does not occur and organization of the endoplasmic reticulum is aberrant, indicative of a disruption in membrane trafficking. The *car-1* gene has homologues in a number of species, including proteins that associate with RNA binding proteins. CAR-1 localizes to P-granules (germ-line specific ribonucleoprotein particles) and discrete, developmentally regulated cytoplasmic foci. These foci also contain DCAP-1, a protein involved in decapping mRNAs. Thus, CAR-1, a protein likely to be associated with RNA metabolism, plays an essential role in the late stage of cytokinesis, suggesting a novel link between RNA, membrane trafficking and cytokinesis in the *C. elegans* embryo.

INTRODUCTION

Recent genetic and proteomic screens have identified a diversity of components needed for cytokinesis including molecular motors, chromosomal passenger proteins, members of membrane trafficking pathways, and components of RNA splicing (Zipperlen *et al.*, 2001; Kamath *et al.*, 2003; Kittler *et al.*, 2004; Skop *et al.*, 2004). These screens have revealed a variety of genes that are required for the execution of the terminal phase of cytokinesis (scission), where the intercellular canal is broken and the membranes of the daughter cells resealed. The number and diversity of these genes suggest that scission probably involves the coordinated activity of several basic processes. The gene Y18D10A.17 (GenBank CAA22317.1) was categorized in an RNAi screen as exhibiting cytokinesis defects (Zipperlen *et al.*, 2001) but no further analysis was performed. This gene has been named *car-1* for cytokinesis (is essential for cytokinesis in the early embryo), apoptosis (plays a role in apoptosis in the germline; Boag *et al.*, 2005), and RNA (associates with RNA-containing structures). We present data that show that CAR-1, a protein whose homology and localization suggest a strong link to RNA processing, plays a crucial role in executing this final phase of cytokinesis and in organizing the endoplasmic reticulum in the early *Caenorhabditis elegans* embryo.

car-1 encodes a predicted protein of 340 amino acids with a glycine-rich region near the C-terminus that includes several clustered RGG (and similar) motifs suggestive of an RGG box (Burd and Dreyfuss, 1994). RGG boxes are found in numerous RNA-binding proteins, although usually in combinations with other RNA-binding motifs. CAR-1 belongs to a family of novel Sm-like proteins (Albrecht and Lengauer, 2004) and homologues of CAR-1 in other species, including the amphibian RAP55 (RNA-associated protein of 55 kDa; Lieb *et al.*, 1998; 46% identical over 337 aa), yeast Scd6p/Lsm13p (suppressor of clathrin deficiency 6-like Sm protein; Nelson and Lemmon, 1993; 31% identical over 316 aa), fly Trailer Hitch (51% identical over 336 aa), and human C19orf13 (34% identical over 319 aa). The similarity of CAR-1 to RAP55 and Scd6p/Lsm13p suggests an association of this protein with RNA metabolism and/or membrane trafficking. The homology of CAR-1 to Scd6p/LSM13p, in the context of the late cytokinesis failure in *C. elegans*, suggests that CAR-1 may provide a link between membrane trafficking pathways and the final stages of cytokinesis worthy of investigation.

MATERIALS AND METHODS

Nematode Strains and Culture Conditions

C. elegans strains were cultured using standard techniques (Brenner, 1974; Sulston and Hodgkin, 1988). Wild-type strain N2 and most GFP-expressing

This article was published online ahead of print in *MBC in Press* (http://www.molbiolcell.org/cgi/doi/10.1091/mbc.E05–09–0874) on November 2, 2005.

[D] [V] The online version of this article contains supplemental material at *MBC Online* (http://www.molbiolcell.org).

Address correspondence to: John G. White (jwhite1@wisc.edu).

Abbreviations used: RNAi, dsRNA interference; RNP, ribonucleoprotein; ER, endoplasmic reticulum.

strains were maintained at 20°C, except the GFP::ZEN-4 strain, which was kept at 25°C. GFP strains included: GFP::αtubulin (C. Malone, strain shared before publication), GFP::ZEN-4 (Kaitna *et al.*, 2000), GFP::SPD-1 (Verbrugghe and White, 2004), GFP::H2B (histone; Praitis *et al.*, 2001), and GFP::SP12 (Poteryaev *et al.*, 2005). A plasmid expressing GFP::CAR-1 was generated as previously described (Verbrugghe and White, 2004) by cloning the full-length genomic DNA for *car-1* in the vector pFJ1.1. The expression of the GFP-tagged CAR-1 was driven by a *pie-1* promotor and UTRs (for early embryo expression), whereas *unc-119*(+) in the vector served as a marker for transformation. A stable transformant expressing GFP::CAR-1 was generated via biolistic transformation (Praitis *et al.*, 2001). For CAR-1 localization in *pgl-1* mutant embryos, the GFP::CAR-1 expressing strain was crossed with *pgl-1*(*ct131*) worms (Kawasaki *et al.*, 2004) provided by Susan Strome. Worms from this cross were maintained at 16°C. L4 hermaphrodites were placed at 25°C overnight before examination of embryos. The *car-1*(*tm1753*) deletion mutation was obtained from the National BioResource Project in Japan (Mitani lab). The mutation site is 124580/124581–125218/125219, resulting in a 628-base pair deletion that spans a portion of exon 2 and all of exon 3. We balanced this deletion mutation over the HT2GFP chromosome (Wang and Kimble, 2001).

RNAi Treatment

car-1 RNAi was performed using the feeding method (Timmons *et al.*, 2001) and embryonic lethality approached 100% after 36 h. L4 animals were fed for 30–48 h at 20°C on bacteria expressing dsRNA for the Y18D10A.17 gene (Zipperlen *et al.*, 2001), with the exception of ZEN4::GFP worms which were fed for 24–30 h at 25°C. RNAi of *zen-4* was also performed via the feeding method, with L4 animals fed for 24–30 h at 20°C before examination. RNAi of *dcap-1* (Y55F3AM.12) performed either via the ingestion method (Kamath *et al.*, 2003) or by injection of dsRNA into the hermaphrodite gonad (Fire *et al.*, 1998) at a concentration of ~1.25 μg/μl. Embryos were examined 48 h after treatment. Both methods yielded the same results.

mCAR-1::GFP Construction and Localization

STO cells (ATCC, Manassas, VA) are an established cell line derived from mouse embryonic fibroblasts. These cells were cultured in 10% calf serum and DMEM (Invitrogen, Carlsbad, CA). The mouse embryonic stem (ES) cell line used was HM1 (Magin *et al.*, 1992). These ES cells were grown in 15% fetal calf serum and DMEM. The mCAR-1::GFP fusion expression vector was made by generating a PCR product using ES cell cDNA (from ES cell total mRNA) as a template and primers designed from the sequence of the predicted CAR-1 homologue in mice (2700023B17Rik, Accession number NM_025948). The full-length PCR product was cloned into the pEGFP-N1 expression vector (Clontech, Palo Alto, CA). This plasmid was used to transiently transfect mouse ES cells, mouse fibroblasts (STO cells), normal murine mammary (NMuMG) (ATCC) cells, and NIH Swiss 3T3 (ATCC) cells using Lipofectamine-mediated gene transfer (Invitrogen). The pEGFP vector only transfection served as a control. Twenty-four hours after transfection, cells were fixed for 15 min in 4% paraformaldehyde (Fisher Scientific, Fair Lawn, NJ), rinsed, and mounted in Vectashield (Vector Laboratories, Burlingame CA). Cells were viewed with a confocal microscope (MRC600; Bio-Rad, Hercules CA).

Antibody Production

Rabbit polyclonal antibodies were generated against bacterial-expressed full-length CAR-1::GST. Protein production, antibody production, and affinity purification were performed by Proteintech Group (Chicago, IL). Rabbit polyclonal antibodies for DCAP-1 were generated against a GST-fusion protein (amino acids 1–333) of DCAP-1 (sequence name Y55F3AM.12, GenBank AC024826), which is 22, 27, and 28% identical to *Saccharomyces cerevisiae* Dcp1p, human DCP1A, and human DCP1B, respectively, in the region comprising the Pfam Dcp-1-like decapping family group. Animal inoculations and serum collection were performed by Cocalico Biologicals (Reamstown, PA).

Labeling

Antibody Labeling. Embryos were labeled with antibodies using the freeze/crack method (Sulston and Hodgkin, 1988) and fixation in 100% methanol (Fisher Scientific). Primary antibody incubation was overnight at 4°C, in 0.5% BSA (Sigma, St. Louis, MO) in PBST (phosphate-buffered saline [PBS] + 0.25% Tween 20; Sigma). Secondary antibody incubation (1:200) was 2 h at room temperature in PBST. Primary antibodies used were rabbit αCAR-1 (1:10 or 1:50); rabbit αDCAP-1 (1:1000 or 1:5000); rabbit αPGL-1 (1:10,000 provided by Susan Strome's lab; Kawasaki *et al.*, 1998); and mouse αtubulin (1:100 DM1α from Sigma). Secondary antibodies used were conjugated with either Alexa488 or Alexa568 (Molecular Probes, Eugene, OR). For propidium iodide (PI) labeling, methanol-fixed embryos were incubated for 20 min in PI (0.1 μg/ml in PBS; Sigma).

Membrane Labeling. Labeling of membrane of living embryos was achieved by puncturing the eggshell using a laser microbeam (Mohler *et al.*, 1998; Wokosin *et al.*, 2003), permitting the ingression of the bath medium: egg buffer (118 mM NaCl, 48 mM KCl, 3 mM $CaCl_2$, 3 mM $MgCl_2$, 5 mM HEPES, pH 7.2; Sigma) containing 100 μM FM 2-10 (Molecular Probes).

Microscopy

4D recording of live embryos using Nomarski optics were performed as previously described (Thomas *et al.*, 1996; Skop *et al.*, 2001). Time-lapse recordings of fluorescently labeled living embryos were collected as previously described (Mohler and Squirrell, 2000; White *et al.*, 2001) using multiphoton microscopy (Wokosin *et al.*, 2003). Fluorescently labeled fixed tissue (GFP or antibody) were mounted in Vectashield (Vector Laboratories) and examined with either confocal microscopy (MRC 600; Bio-Rad) or multiphoton microscopy using 890-nm wavelength (effective excitation ~445 nm) and a 480- to 550-nm bandpass filter for the green emission and a 580-nm long pass filter for the red emission. Data were viewed and analyzed with ImageJ (Wayne Rasband, http://rsb.info.nih.gov/ij/).

Quantitation

To determine the change in the population of puncta with development, the number of small GFP::CAR-1 puncta were counted in a single optical plane at different developmental stages in living embryos imaged with multiphoton microscopy. The area of the embryo in which the puncta were counted was used to generate the puncta/μ^2 value. To determine the number of CAR-1 puncta containing DCAP-1, puncta were counted in fixed embryos (4–16 cell stage) expressing GFP::CAR-1 and labeled with αDCAP-1 antibody. A single optical plane was analyzed per embryo, with the P-cell being eliminated from the analysis to prevent confusion with P-granule labeling.

RESULTS

Embryos With Suppressed car-1 Expression Lack a Midzone and Fail in Late Cytokinesis

Reduced expression of the gene *car-1* causes a failure of the late stage of cytokinesis in the *C. elegans* embryo Time-lapse recordings using Nomarski microscopy showed that cleavage furrows in the one cell embryo initiated and ingressed (full ingression = 71%; partial ingression = 27%; no ingression = 2%; N = 56), but then subsequently regressed (69% regressed immediately; 25% regressed with some delay; 5% did not regress; N = 55; Figure 1A). Additional abnormalities evident during the first cell cycle included erratic movements of pronuclei during centration (45%, N = 33), violent rocking of the mitotic spindle (79%, N = 56), and extra nuclei (38%, N = 48). Embryos from adults homozygous for *car-1*(*tm1753*), a deletion mutation (Figure 1A), exhibit phenotypes similar to those observed in *car-1(RNAi)* embryos, indicating that these are probably loss of function defects (pronuclear wobble = 66%, N = 6; violent spindle movements = 83%, N = 6; first division failure = 90%, N = 10; furrow fully ingressed before failure = 83%, N = 6). Depletion of CAR-1 did not affect other early embryonic events, such as the establishment of polarity: the localization of GFP::PAR-2, PIE-1::GFP, and GFP::NMY-2, proteins which exhibit polarized distribution in the early embryo, was not disrupted in *car-1*(*RNAi*) embryos (unpublished data). Adult animals grown for longer than 48 h on RNAi feeding bacteria became sterile, suggesting possible defects in germline development and/or gametogenesis.

To further examine the cytokinesis failure, we observed plasma membrane dynamics using the membrane probe FM 2-10 (Mohler *et al.*, 1998). The accumulation of membrane that develops on the late furrow in wild-type embryos (Skop *et al.*, 2001) did not occur in *car-1*(*RNAi*) embryos (Figure 1B and Supplementary Movies 1 and 2), indicating an abnormality in membrane trafficking to the late furrow. To determine the origin of extra micronuclei that were occasionally observed, we examined chromosome separation at anaphase in *car-1*(*RNAi*) embryos using a GFP::histone reporter (Praitis *et al.*, 2001). Some chromosome separation abnormalities were seen, such as lagging or broken chromosomes (85%, N = 7; Figure 2A). However, cleavage failures oc-

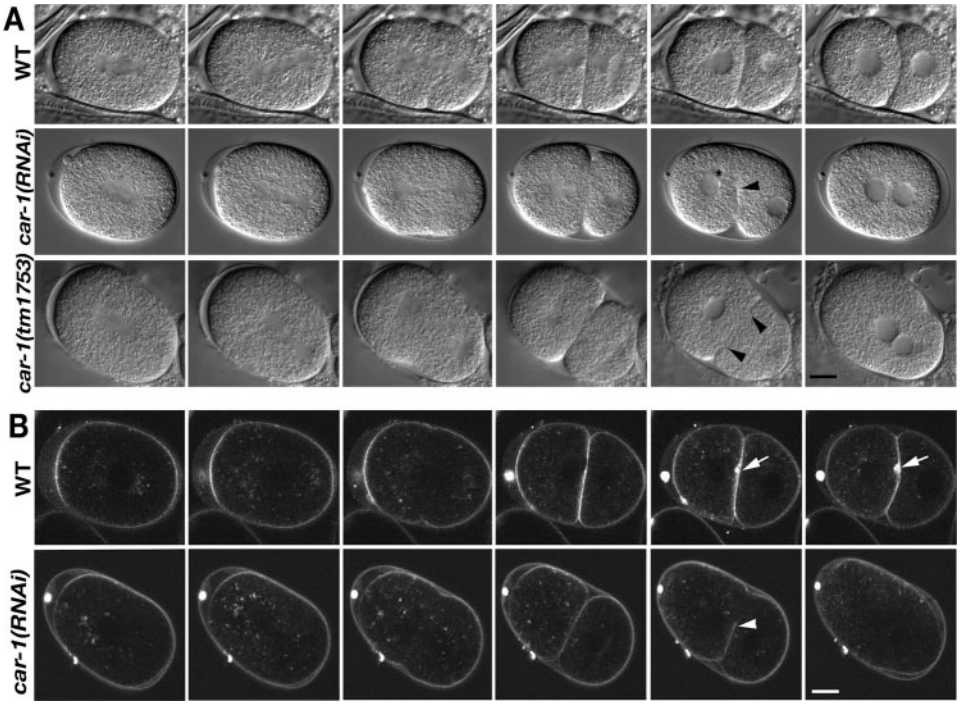

Figure 1. CAR-1 depleted embryos fail late cytokinesis. Each time sequence illustrates the following developmental stages, from left to right: spindle formation; spindle elongation; further spindle elongation/cleavage furrow initiation; cleavage furrow completion; early 2-cell/cytokinesis failure; late 2 cell. (A) Top row is a wild-type embryo. Nomarski images showing that the depletion of CAR-1, either by RNAi (middle row) or a deletion mutation (*car-1(tm1735)*) (bottom row) caused the cleavage furrow to regress (black arrowhead) after it had fully ingressed. Asterisk denotes extra micronucleus in RNAi treated embryo. (B) In the wild-type embryo (top row) labeled with the membrane dye FM 2-10, there was a striking accumulation of membrane, after the complete ingression of the cleavage furrow, at the scission site (white arrow), which persisted through much of the cell cycle; no such accumulation was seen in the *car-1*(*RNAi*) embryo (bottom row). Instead, the membrane regressed (white arrowhead). For this and all other embryo figures, anterior is toward the left. Scale bar, 10 μm.

curred in embryos without evident defects in chromosome segregation, indicating that segregation defects per se were not the primary cause of scission failures. Previous studies have shown that chromosome segregation failures do not necessarily result in cytokinesis failures (O'Connell *et al.*, 1998; Severson *et al.*, 2000).

To determine the effect of CAR-1 depletion on spindle function, we examined GFP::tubulin dynamics in *car-1*(*RNAi*) embryos using time-lapse multiphoton microscopy and observed a conspicuous lack of the tightly bundled microtubules that form the midbody (Powers *et al.*, 1998), although astral microtubules appeared normal (Figure 2B and Supplementary Movies 3 and 4). The spindle poles of these *car-1*(*RNAi*) embryos separated further in anaphase than in wild type (Figure 2E), a phenotype consistent with the lack of a spindle midzone holding the centrosomes together during anaphase B (Grill *et al.*, 2001; Verbrugghe and White, 2004).

To further investigate this apparent lack of spindle midzone, we assessed the localization of two spindle midzone components, ZEN-4 (Mishima *et al.*, 2002) and SPD-1 (Verbrugghe and White, 2004) in *car-1*(*RNAi*) embryos. GFP::ZEN-4 localized to metaphase chromosomes, as previously reported for the wild-type embryo (Verbrugghe and White, 2004). After the metaphase to anaphase transition, GFP::ZEN-4 dissociated from the chromosomes and associated with some of the microtubules in the midzone region (Figure 2C) but was less focused than in wild type. Although *car-1*(*RNAi*) embryos did not exhibit the wild-type accumulation of GFP::ZEN-4 in the spindle midbody at late telophase (Powers *et al.*, 1998; Raich *et al.*, 1998), GFP::ZEN-4 did associate with the cleavage furrow (Figure 2C) as also occurs in the wild type (Verbrugghe and White, 2004). GFP::SPD-1 behaved similar to GFP::ZEN-4. It rapidly associated with microtubules at the metaphase to anaphase transition, as in the wild type, but did not accumulate at the spindle midbody. However, GFP::SPD-1 did localize normally to cytoplasmic microtubules (Figure 2D). Thus the cell-cycle-regulated association of ZEN-4 and SPD-1 to microtubules at anaphase onset occurred normally in *car-1*(*RNAi*) embryos but the dense association of these proteins usually seen at the midbody at telophase was absent. These observations suggest that the defects caused by CAR-1 depletion are not general microtubule defects but rather are specific to the spindle midzone.

CAR-1 Localizes to Cytoplasmic Puncta

We localized CAR-1 in embryos using both an antibody prepared against bacterially expressed CAR-1 as well as a reporter expressing GFP::CAR-1. Fluorescence signals of both GFP::CAR-1 and the antibody labeling were extinguished in *car-1*(*RNAi*) embryos, thereby demonstrating the specificity of the reagents (Supplementary Figure 1, A and B). CAR-1 localized diffusely throughout the cytoplasm, weakly to the mitotic spindle in the GFP::CAR-1 strain and strongly to large and small puncta (mean large = 1.0 $\pm$ 0.3 μm; mean small = 0.5 $\pm$ 0.1 μm; N = 8 embryos and 40 puncta of each category; Figure 3A).

Only a few small CAR-1 containing puncta were seen in the one cell embryo and the interphase 2-cell embryo. However, there was a dramatic increase in the number of small puncta during and after the division of the anterior (AB) cell (Figure 3A and Supplementary Movie 5), whereas the diffuse cytoplasmic signal decreased with subsequent cell divisions. The population of these smaller puncta did not noticeably change in a cyclical manner, suggesting that they are not under cell cycle regulation. The mouse homologue of CAR-1 (34% identical over 319 aa; a predicted gene of unknown function) tagged with GFP exhibited a similar punctate pattern in ES cells, fibroblasts (STO; Figure 3B), mammary cells (NMuMG), and Swiss 3T3 cells (unpublished data), indicating that the intracellular distribution, and thus possibly function, of this protein is conserved.

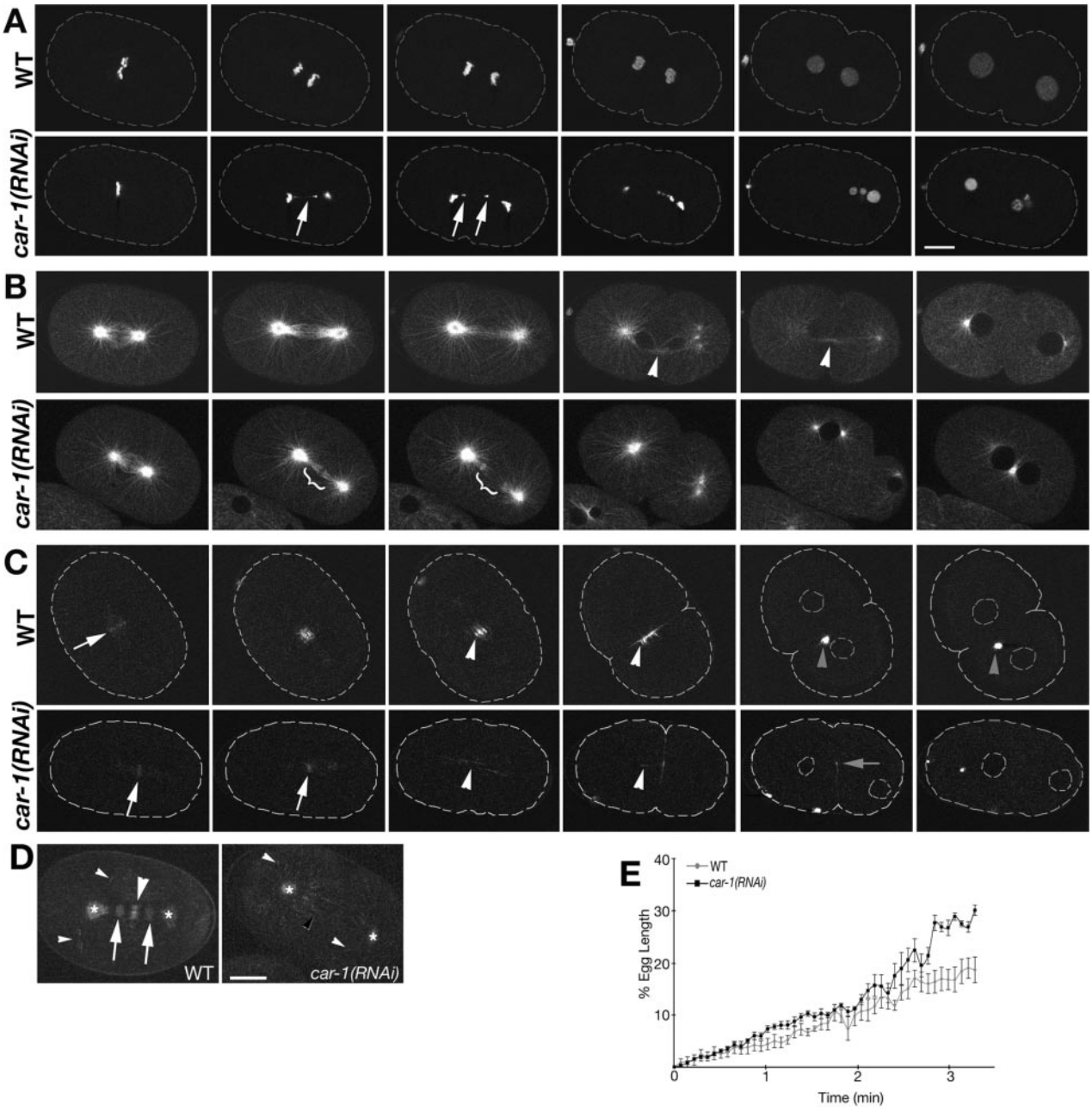

Figure 2. CAR-1 depleted embryos exhibit spindle midzone defects. Each multiphoton time sequence (A–C) illustrates the following developmental stages, from left to right: spindle formation; spindle elongation; further spindle elongation/cleavage furrow initiation; cleavage furrow completion; early 2-cell/cytokinesis failure; late 2 cell. For each series, top row is a wild-type embryo and the bottom row is a *car-1*(*RNAi*) embryo. (A) GFP::Histone expressing embryos treated with *car-1*(*RNAi*) exhibited lagging chromosome fragments during spindle elongation (white arrow), resulting in micronuclei. (B) In the control GFP::tubulin expressing embryo a prominent and persistent midbody was observed as the cleavage furrow completed (white arrowhead), which was absent in the *car-1*(*RNAi*) embryo. Also the spindle microtubule bundle became radially compressed compared with the control embryo during early elongation, giving the appearance of a thinner spindle, which seemed to ultimately break (bracket). (C) GFP::ZEN-4 localized to metaphase chromosomes in the *car-1*(*RNAi*) embryo, as it did in the control (white arrow). ZEN-4 moved to midzone microtubules in the RNAi treated embryo, as in the control (white arrowhead), but did not properly organize into a midbody structure (gray arrowhead in wild-type embryo). However, it did localize to the cleavage furrow, even as the cleavage furrow regressed (gray arrow). Bright spot in last image is an internalized remnant from the meiotic division. Dashed lines for GFP::ZEN4 and GFP::Histone sequences are embryo outlines taken from the corresponding brightfield images (unpublished data). (D) These images are projections of 10 time points (4 s apart) showing the localization SPD-1 during spindle elongation. In the control embryo, SPD-1 localized to the reforming nuclei (white arrows), the spindle midzone (large white arrowhead), centrosomes (asterisk), and cytoplasmic microtubules (small white arrowhead). *car-1*(*RNAi*) embryo showed the same localizations (nuclei not shown in this plane) except the microtubule labeling in the midzone region was more dispersed (small black arrowhead), resembling the cytoplasmic microtubule labeling. Scale bars, 10 μm. (E) The average change in spindle length is illustrated, in wild-type and in *car-1*(*RNAi*) embryos, measured as a percentage of egg length, showing that a greater change in the spindle length in the *car-1*(*RNAi*) embryos than in the untreated embryos, particularly later in elongation. The points are averages of three untreated or four *car-1*(*RNAi*) embryos expressing GFP::tubulin, with SEM shown for each point. Time 0 is the initiation of chromosome separation and measurements were taken at 4.37-s intervals.

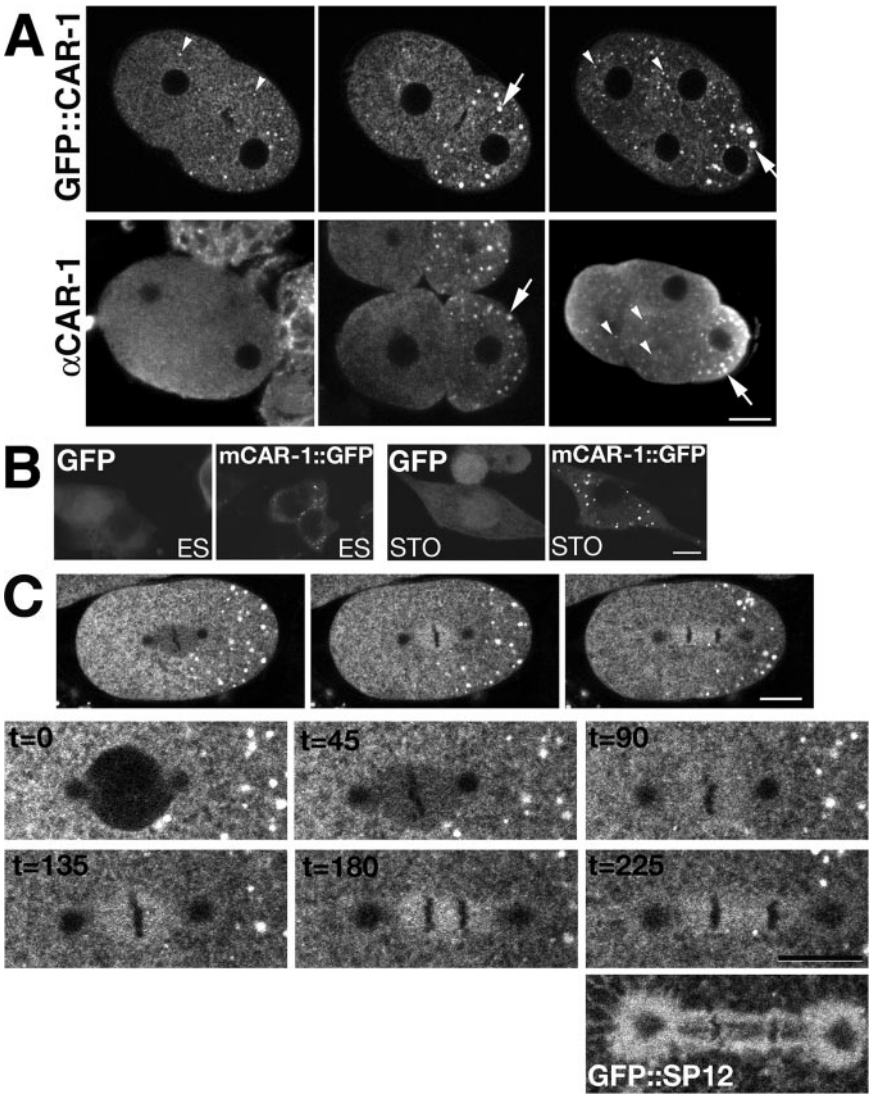

Figure 3. CAR-1 localizes to cytoplasmic puncta and can associate with the anaphase spindle. (A) Columns indicate the following developmental stages: pronuclear migration, 2-cell interphase, and 4-cell interphase. The top row is a multiphoton time sequence of a living embryo showing changes in distribution of GFP::CAR-1, with few small cytoplasmic puncta (small arrowhead) present during pronuclear migration and larger puncta developing in the posterior during and after cytokinesis (arrow). There was an increase in the number of small cytoplasmic puncta during and after the 2–4 cell division; midpronuclear migration: 0.007 ± 0.004 puncta/μ^2, N = 4 embryos; 2-cell interphase: 0.004 ± 0.003 puncta/μ^2, N = 8 embryos; AB furrow initiation: 0.013 ± 0.004 puncta/μ^2, N = 8 embryos; interphase Aba = 0.038 ± 0.007. An antibody to CAR-1 showed a similar pattern in fixed embryos (bottom row). (B) Confocal images of mouse embryonic stem cells (ES) or fibroblasts (STO) transfected with either GFP only or with the full-length mCAR-1 tagged with GFP. The mCAR-1::GFP was expressed in numerous discrete foci in both embryonic stem cells and in fibroblasts. (C) Multiphoton time series of living embryos showing CAR-1 spindle localization. GFP::CAR-1 was initially absent from the spindle and then accumulated on the spindle region, and as the spindle elongated, the CAR-1 label extended along the spindle to include the pericentriolar region. Lower series shows an enlargement of the spindle region at 45-s intervals, with the final image compared with the organization of the ER (lowest image shows GFP::SP12). These images were taken with higher detector gain than those in A to accentuate the nonpunctate cytoplasmic distribution of GFP::CAR-1. Scale bars, 10 μm.

In addition to the strongly labeled puncta, labeled CAR-1 could be found in the spindle region during mitosis (Figure 3C, Supplementary Movie 6) in live *C. elegans* embryos. The intensity of this signal increased as mitosis progressed and, as the chromosomes separated, the signal extended along the elongating spindle to include the pericentriolar region, resembling the organization of the ER (Poteryaev *et al.*, 2005; Figure 3C).

Large CAR-1 Puncta Are P-Granules and the Small Puncta Are Putative Cytoplasmic RNA-processing Sites

The large CAR-1 puncta were confined to the germplasm and colocalized with PGL-1 (Figure 4A), a component of P-granules (Kawasaki *et al.*, 1998). P-granules are ribonuclear protein (RNP) particles that segregate asymmetrically in the embryo, accumulate in the germplasm, and are essential for germline development (Strome and Wood, 1983). Although *car-1*(*RNAi*) embryos were abnormal because of the cytokinesis defect, and PGL-1 labeling was somewhat more diffuse, suggestive of some effect of CAR-1 depletion on PGL-1 localization, PGL-1 was still found in large, posteriorly localized granules (Figure 4B). Similarly, GFP::CAR-1 localized properly in *pgl-1*(*ct131*) mutants (Figure 4B). Thus, PGL-1 and CAR-1 localization to P-granules are not codependent. Other P-granule components have been found to localize independently of each other, even when they coimmunoprecipitate or interact in a yeast two-hybrid assay (Kawasaki *et al.*, 2004).

The small CAR-1 containing foci did not label with the αPGL-1 antibody (Figure 4B). The similarity of CAR-1 to the *Xenopus* RNP protein Rap55, along with its localization to P-granules, suggest that these small puncta may be sites of RNA storage and/or processing. We found that CAR-1-positive particles also labeled with the nucleic acid label PI (Figure 4C), indicating that these small puncta, as well as the P-granules, contain RNA. This pattern of cytoplasmic PI labeling was clearly distinct from the published pattern of mitochondria organization (Badrinath and White, 2003).

The presence of RNA in the small CAR-1 puncta imply a resemblance to the cytoplasmic "processing bodies" (P-bodies) of yeast (Sheth and Parker, 2003) and cytoplasmic foci of human cells involved in mRNA turnover and include the decapping complex component, DCP1 (van Dijk *et al.*, 2002; Cougot *et al.*, 2004). To investigate the possibility that the small CAR-1-containing puncta are analogous to P-bodies, we labeled embryos with an antibody to *C. elegans* homo-

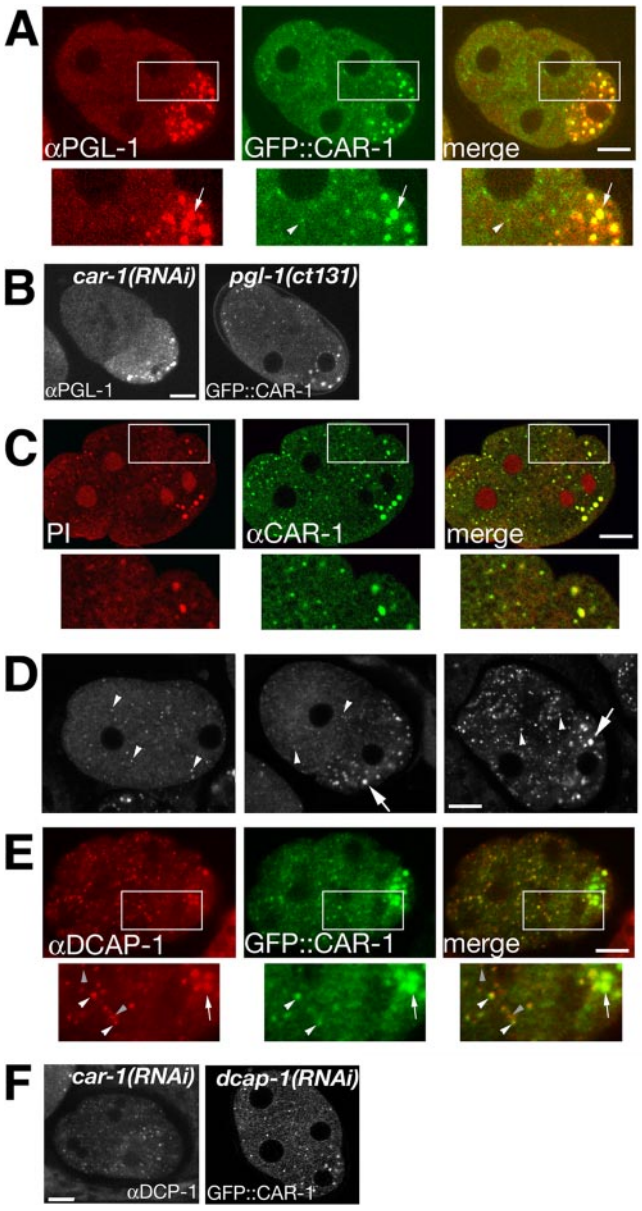

Figure 4. CAR-1 localizes with P-granules and particles containing RNA and DCAP-1. (A) Confocal images showing that the large puncta (white arrows) of GFP::CAR-1 (green) colocalized with the P-granule component PGL-1 (red), whereas the small puncta (white arrowhead) did not. (B) PGL-1 was present in CAR-1-depleted embryos and, conversely, GFP::CAR-1 was not disrupted in the *pgl-1* mutant. Designations in bold at the top of each image indicate genotype while designation at bottom of each image indicate label. (C) Multiphoton microscopy images showing that both small and large CAR-1 punta (green) label with propidium iodide (PI; red). (D) Confocal micrographs showing the localization of DCAP-1 in large and small cytoplasmic puncta (top row: pronuclear migration, 2-cell interphase, 4-cell interphase). (E) Both the large (white arrow) and small (white arrowhead) CAR-1 puncta (green) colocalized with DCAP-1-positive puncta (red); however, some DCAP-1 puncta appear to lack clear CAR-1 signal (gray arrowhead). (F) DCAP-1 was present when CAR-1 was depleted by RNAi, and GFP::CAR-1 expression was present in *dcap-1*(*RNAi*) embryos. Scale bars, 10 μm.

logue of DCP1, DCAP-1. DCAP-1 localized diffusely throughout the cytoplasm, with prominent concentrations of signal in discrete cytoplasmic foci (Figure 4D), which was absent in *dcap-1*(*RNAi*) embryos (Supplementary Figure 1). DCAP-1 puncta were numerous during pronuclear migration, when CAR-1 foci were few in number (see above). After pronuclear centration two populations of DCAP-1 foci were evident: large particles that segregated to the posterior cell and smaller puncta scattered in the cytoplasm of both cells. The large foci contained PGL-1 (unpublished data), identifying them as P-granules. The small DCAP-1-containing foci colocalized with CAR-1 (Figure 4E). Not all DCAP-1 puncta label with GFP::CAR-1 although most small CAR-1 puncta labeled with αDCAP-1 (DCAP-1 only = 67%; CAR-1 only = 2%; both DCAP-1 and CAR-1 = 31%; N = 1014 puncta in 12 embryos). DCAP-1 localization was unaltered in *car-1*(*RNAi*) embryos and CAR-1 localization was unaltered in *dcap-1*(*RNAi*) embryos (Figure 4F), indicating that each does not require the presence of the other for localization. RNAi depletion of DCAP-1 did not result in cytokinesis defects (unpublished data), suggesting that the role of CAR-1 in cytokinesis may not directly involve this decapping protein. However, the presence of DCAP-1 in CAR-1 puncta suggests that the puncta are, indeed, similar to RNA decay particles described in yeast and human cells.

CAR-1 Puncta Associate with ER Structures and Depletion of CAR-1 Disrupts ER Organization

The homology of CAR-1 to Scd6/Lsm13 in yeast suggests a possible link between CAR-1 and membrane dynamics. This connection is supported by our observation that CAR-1 depletion prevented the accumulation of membrane at the scission site after cytokinesis (Figure 1B). The ER undergoes distinct cell cycle-dependent organizational changes in the *C. elegans* embryo that correlate with cytokinesis and are independent of microtubules (Poteryaev *et al.*, 2005). When embryos expressing GFP::SP12, an ER protein (Poteryaev *et al.*, 2005), were labeled with the CAR-1 antibody, an association of CAR-1 puncta with ER structures was observed. We found that the small CAR-1 puncta were generally situated on or next to ER structures (Supplementary Figure 2). More compelling is the functional link between CAR-1 and ER dynamics. In wild-type embryos, the organization of the ER cycles in a distinct, cell cycle-dependent manner between a "dispersed" state during interphase to a highly ordered "reticulate" state during mitosis, which rapidly disassembles as the cleavage furrow ingresses (Poteryaev *et al.*, 2005; Figure 5, Supplementary Movie 7). This organization was disrupted in *car-1*(*RNAi*) embryos, even before the onset of cytokinesis. Although some indications of the reticulate organization could be identified in mitotic *car-1*(*RNAi*) embryos (Figure 5, Supplementary Movie 8), the reticulation was not as well formed as in nontreated embryos, with much of the ER existing as abnormal diffuse patches or thick strands. The spindle and midzone associated ER was sparse in *car-1*(*RNAi*) embryos (Figure 5). Abnormal patches and strands of ER were also present after mitosis, when the ER returned to a dispersed state.

To assess whether this disrupted organization of the ER was specific to the depletion of CAR-1 rather than a general consequence of an aberrant midzone and/or cytokinesis failure, we examined the ER in *zen-4*(*RNAi*) embryos, which also lack a spindle midzone and fail in scission (Powers *et al.*, 1998; Raich *et al.*, 1998). We found that although these embryos did lack significant accumulation of ER in the spindle midzone region, both the reticulate and dispersed organizations of ER were unperturbed and the extensive ER patches and thick strands found in *car-1*(*RNAi*) embryos were absent (Figure 5). These data show that the absence of CAR-1 disrupted ER organization and this disruption was not a

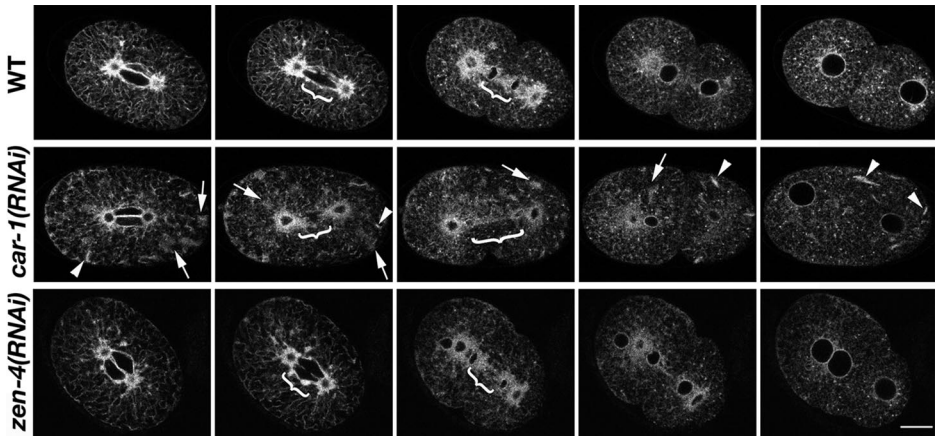

Figure 5. CAR-1 depletion disrupts the organization of the ER. (A) Multiphoton time series of living embryos showing ER dynamics. Sequences illustrate the organization of the ER (visualized by GFP::SP12; Poteryaev *et al.*, 2005) during premetaphase, metaphase, anaphase, telophase, and interphase (2-cell stage). In the control embryo (top row), the ER outlined the spindle and exhibited a distinct reticulate structure. This structure became dispersed as the cleavage furrow ingressed and the cell entered interphase. CAR-1 depletion (second row) perturbed ER reticulation during mitosis, causing patchy accumulations (arrows) or thick strands (arrowheads) of ER that persisted into interphase. The *car-1*(*RNAi*) embryo also showed a reduction in spindle associated ER in the midzone region (bracket) during mitosis progression. Although the *zen-4*(*RNAi*) embryo did have somewhat reduced midzone ER during anaphase, unlike the *car-1*(*RNAi*) embryo, substantial ER was still present near the reforming nuclei (bracket, middle panel) and the ER formed normal looking reticulate structures during metaphase. Scale bar, 10 μm.

result of the cytokinesis failure. Furthermore, embryos treated with brefeldin A (BFA), which disrupts secretion (Orci *et al.*, 1991) and causes cytokinesis failures in *C. elegans* embryos (Skop *et al.*, 2001), did not alter the localization of CAR-1 (Supplementary Figure 3), indicating that CAR-1 localization is not dependent upon BFA-sensitive vesicle trafficking.

DISCUSSION

In the *C. elegans* embryo, CAR-1 localized throughout the cytoplasm and accumulated in two discrete populations of foci. First, CAR-1 colocalized with PGL-1-positive P-granules, which contain RNA (Pitt *et al.*, 2000; Schisa *et al.*, 2001) along with specific RNA helicases (Gruidl *et al.*, 1996). Similar mRNP particles are found in the germ plasm of many species and are likely involved in mRNA storage and metabolism in the early embryo (Bashirullah *et al.*, 2001; de Moor and Richter, 2001; Johnstone and Lasko, 2001). Second, CAR-1 localized to small cytoplasmic foci that contained RNA and DCAP-1. Such foci may be analogous to yeast and mammalian mRNA processing bodies. DCAP-1 containing puncta were evident from the earliest stages of embryogenesis in *C. elegans* but CAR-1 did not localize to significant numbers of these foci until the AB cell divided, indicating that the processing body association of CAR-1 is temporally regulated. Although CAR-1 contains several clustered RGG motifs, it does not contain other obvious RNA-binding domains, a feature of most RGG-box RNA-binding proteins (Burd and Dreyfuss, 1994), suggesting that CAR-1 does not directly bind RNA but may be an adaptor protein for proteins that do bind RNA. Because the assimilation of maternal mRNAs into the translational pool, as well as their subsequent turnover, are highly regulated (Seydoux, 1996), one function of CAR-1 may be to deliver certain mRNAs to the processing bodies and could either inhibit or potentiate their degradation at an appropriate time in development. Interestingly, the CAR-1 localization to the putative processing bodies dramatically increased *after* the first cytokinesis, suggesting that this localization is either independent of its role in cytokinesis or CAR-1 may be transporting mRNA(s) that are required for the completion of the first cytokinesis to these sites of turnover in order that they be degraded at the proper time. Alternatively, it is possible that CAR-1 is protecting or processing mRNAs while it is dispersed in the cytoplasm, before its accumulation in foci.

Several proteins involved in RNA metabolism have unexpected roles in cytokinesis (Liu *et al.*, 2002; Makarov *et al.*, 2002; Oeffinger and Tollervey, 2003; Kittler *et al.*, 2004). Recently, work in *Xenopus* egg extracts indicates that RNA may play a translation-independent role in the mitotic spindle, possibly providing stability to the mitotic apparatus (Blower *et al.*, 2005). The authors demonstrate that an mRNA export factor, Rae1, a member of an RNP complex, is important for spindle assembly and can associate with Rap55, the *Xenopus* homologue of CAR-1. This observation supports the possibility that the presence of CAR-1 in the anaphase spindle could regulate the integrity of the spindle midbody.

We demonstrate that reduced expression of CAR-1 in the *C. elegans* early embryo leads to highly penetrant defects in scission. The failure of these embryos to form a spindle midbody may, at least in part, explain the cytokinesis failures. However, a spindle midbody may not be strictly required for successful cytokinesis in the early *C. elegans* embryo (Bringmann and Hyman, 2005) provided midzone components are present on the advancing furrow (Verbrugghe and White, 2004). ZEN-4 was present on the cleavage furrow of *car-1*(*RNAi*) embryos, suggesting that the lack of the spindle midzone alone may not be a sufficient explanation for the scission failures in *car-1*(*RNAi*) embryos. The absence of membrane accumulation at the scission site, along with alterations in ER organization, show that the lack of CAR-1 perturbs membrane dynamics. Because a role for membrane trafficking in scission has been identified (Skop *et al.*, 2001; Low *et al.*, 2003), the lack of membrane traffic to the apex of the late cleavage furrow in CAR-1 depleted embryos could explain the cytokinesis defect. The scission failures and ER organization of *car-1*(*RNAi*) embryos are reminiscent of those induced by BFA, which inhibits Golgi-derived membrane traffic (Skop *et al.*, 2001, Poteryaev *et al.*, 2005). In both *car-1*(*RNAi*) and BFA-treated embryos the striking accumulation of membrane that normally occurs at the scission site is absent and the ER does not undergo its proper structural changes.

A direct role for CAR-1 in membrane trafficking is suggested in budding yeast by the observation that elevated expression of Scd6p/LSM13p, the homologue of CAR-1, suppresses the lethal phenotype associated with clathrin

deficiency (Nelson and Lemmon, 1993). We observed that the distribution of GFP::CAR-1 at anaphase resembled the organization of the ER around the spindle at this time. Time-lapse video recordings suggest that some small puncta may originate from this spindle region (Supplementary Movie 6). The ARF-1 GTPase regulates COPI vesicle budding from the Golgi to the ER. Inhibition of ARF-1 by RNAi or BFA treatment causes changes of ER appearance (Poteryaev *et al.*, 2005) that are similar, although not identical, to those seen with *car-1*(*RNAi*). Additionally, disruption of Axs, a protein that colocalizes with ER ensheathing the spindle in *Drosophila*, causes spindle assembly defects (Kramer and Hawley, 2003). Because one of the key functions of the ER is to regulate levels of free cytoplasmic calcium (Putney and Ribeiro, 2000), the reduction of ER around the spindle in *car-1*(*RNAi*) embryos may result in a destabilization of the spindle microtubules through high levels of free calcium (Salmon and Segall, 1980), due to a lack of ER calcium buffering, leading to the observed lack of spindle midzone, ultimately causing the failure in cytokinesis. CAR-1 may contribute to the stability of the spindle midzone, possibly by facilitating the accumulation of ER around the spindle midzone. The observation that CAR-1 decorates the mitotic spindle along with the ER, together with evidence in *Xenopus* that RNA and RNPs are important for spindle stability (Blower *et al.*, 2005), suggests that CAR-1, perhaps in conjunction with associated RNA binding proteins and their bound RNAs, is required for regulating the morphology of the ER in the vicinity of the spindle.

We have shown that CAR-1 is required for scission in the early embryo and is associated with RNA processing complexes. Also we show that CAR-1 depletion disrupts the structure of the ER and the spindle midzone after the metaphase to anaphase transition. Recent observations have shown that Trailer Hitch (a homologue of CAR-1 in *Drosophila*) is associated with ER exit points and is required for targeted secretion of Gurken (Wilhelm *et al.*, 2005). Also it has been shown that RNA is important for spindle stability in *Xenopus* (Blower *et al.*, 2005) and RNA complexes can bind membranes directly (Vlassov *et al.*, 2001). We suggest a model as to how CAR-1 may function, probably as part of an RNP complex, to link the three seemingly disparate cellular processes of ER organization, RNA association, and scission site stability. We propose that CAR-1 functions in embryonic cytokineses as part of an RNA-regulated, membrane-associated exit point complex required for spatial differentiation of the ER. In this model, CAR-1 would contribute, at metaphase, to organizing the ER in close association with the mitotic spindle where the ER could regulate the local calcium concentration in the spindle (Parry *et al.*, 2005), allowing the midzone microtubules to remain stable (Salmon and Segall, 1980) at a time when cytoplasmic microtubules are being depolymerized. As the cell transitions into anaphase and telophase, the CAR-1 complex forms exit points (Wilhelm *et al.*, 2005) in the spindle-associated ER where the membrane (Low *et al.*, 2003; Skop *et al.*, 2004) and glycoproteins (Wang *et al.*, 2005) required for completion of cytokinesis can be released at the scission site. At the completion of cytokinesis, specific RNAs required for the cytokinesis exit points are degraded, possibly in a CAR-1-dependent manner, thereby disabling the formation of this ER specialization until the next cell cycle.

ACKNOWLEDGMENTS

We thank Drs. J. Ahringer, J. Austin, C. Malone, M. Glotzer, and S. Strome, for generously providing strains and reagents. We appreciate the work of the Mitani lab as part of the National BioResourse Project in Japan for providing the *car-1*(*tm1753*) strain. We thank K. Verbrugghe for providing GFP::SPD-1 strain as well as assistance with the GFP::CAR-1 construction. We appreciate the expertise of C. Spike on the P-granule evaluation and S. Untawale for assistance with the mammalian cell culture and the laboratory of Dr. P. Keely for the NMuMG cells. We thank K. Verbrugghe and K. Blackwell for comments on the manuscript. We also thank the labs of K. Blackwell, K. Oegema, and J. Wilhelm for sharing data before publication. This work was supported by grant from the National Institutes of Health to J.G.W. (RO1 GM7583) and to P.A. (RO1 GM50933) and a National Research Service Award (5 F32 GM63349-02) to J.M.S.

REFERENCES

Albrecht, M., and Lengauer, T. (2004). Novel Sm-like proteins with long C-terminal tails and associated methyltransferases. FEBS Lett. *569*, 18–26.

Badrinath, A. S., and White, J. G. (2003). Contrasting patterns of mitochondrial redistribution in the early lineages of *Caenorhabditis elegans* and *Acrobeloides sp.* PS1146. Dev. Biol. *258*, 70–75.

Bashirullah, A., Cooperstock, R. L., and Lipshitz, H. D. (2001). Spatial and temporal control of RNA stability. Proc. Natl. Acad. Sci. USA *98*, 7025–7028.

Blower, M. D., Nachury, M., Heald, R., and Weis, K. (2005). A Rae1-containing ribonucleoprotein complex is required for mitotic spindle assembly. Cell *121*, 223–234.

Boag, P., Nakamura, A., and Blackwell, T. K. (2005). A conserved RNA-protein complex component involved in physiological germline apoptosis regulation in *C. elegans.* Development *132*, 4975–4986.

Brenner, S. (1974). The genetics of *Caenorhabditis elegans.* Genetics *77*, 71–94.

Bringmann, H., and Hyman, A. A. (2005). A cytokinesis furrow is positioned by two consecutive signals. Nature *436*, 731–734.

Burd, C. G., and Dreyfuss, G. (1994). Conserved structures and diversity of functions of RNA-binding proteins. Science *265*, 615–621.

Cougot, N., Babajko, S., and Seraphin, B. (2004). Cytoplasmic foci are sites of mRNA decay in human cells. J. Cell Biol. *165*, 31–40.

de Moor, C. H., and Richter, J. D. (2001). Translational control in vertebrate development. Int. Rev. Cytol. *203*, 567–608.

Fire, A., Xu, S., Montgomery, M. K., Kostas, S. A., Driver, S. E., and Mello, C. C. (1998). Potent and specific genetic interference by double-stranded RNA in *Caenorhabditis elegans.* Nature *391*, 806–811.

Grill, S. W., Gonczy, P., Stelzer, E. H., and Hyman, A. A. (2001). Polarity controls forces governing asymmetric spindle positioning in the *Caenorhabditis elegans* embryo. Nature *409*, 630–633.

Gruidl, M. E., Smith, P. A., Kuznicki, K. A., McCrone, J. S., Kirchner, J., Roussell, D. L., Strome, S., and Bennett, K. L. (1996). Multiple potential germ-line helicases are components of the germ-line-specific P granules of *Caenorhabditis elegans.* Proc. Natl. Acad. Sci. USA *93*, 13837–13842.

Johnstone, O., and Lasko, P. (2001). Translational regulation and RNA localization in *Drosophila* oocytes and embryos. Annu. Rev. Genet. *35*, 365–406.

Kaitna, S., Mendoza, M., Jantsch-Plunger, V., and Glotzer, M. (2000). Incenp and an aurora-like kinase form a complex essential for chromosome segregation and efficient completion of cytokinesis. Curr. Biol. *10*, 1172–1181.

Kamath, R. S. *et al.* (2003). Systematic functional analysis of the *Caenorhabditis elegans* genome using RNAi. Nature *421*, 231–237.

Kawasaki, I., Amiri, A., Fan, Y., Meyer, N., Dunkelbarger, S., Motohashi, T., Karashima, T., Bossinger, O., and Strome, S. (2004). The PGL family proteins associate with germ granules and function redundantly in *Caenorhabditis elegans* germline development. Genetics *167*, 645–661.

Kawasaki, I., Shim, Y. H., Kirchner, J., Kaminker, J., Wood, W. B., and Strome, S. (1998). PGL-1, a predicted RNA-binding component of germ granules, is essential for fertility in *C. elegans.* Cell *94*, 635–645.

Kittler, R. *et al.* (2004). An endoribonuclease-prepared siRNA screen in human cells identifies genes essential for cell division. Nature *432*, 1036–1040.

Kramer, J., and Hawley, R. S. (2003). The spindle-associated transmembrane protein Axs identifies a new family of transmembrane proteins in eukaryotes. Cell Cycle *2*, 174–176.

Lieb, B., Carl, M., Hock, R., Gebauer, D., and Scheer, U. (1998). Identification of a novel mRNA-associated protein in oocytes of *Pleurodeles waltl* and *Xenopus laevis.* Exp. Cell Res. *245*, 272–281.

Liu, L., Liang, X. H., Uliel, S., Unger, R., Ullu, E., and Michaeli, S. (2002). RNA interference of signal peptide-binding protein SRP54 elicits deleterious effects and protein sorting defects in trypanosomes. J. Biol. Chem. *277*, 47348–47357.

Low, S. H., Li, X., Miura, M., Kudo, N., Quinones, B., and Weimbs, T. (2003). Syntaxin 2 and endobrevin are required for the terminal step of cytokinesis in mammalian cells. Dev. Cell *4*, 753–759.

Magin, T. M., McWhir, J., and Melton, D. W. (1992). A new mouse embryonic stem cell line with good germ line contribution and gene targeting frequency. Nucleic Acids Res. *20*, 3795–3796.

Makarov, E. M., Makarova, O. V., Urlaub, H., Gentzel, M., Will, C. L., Wilm, M., and Luhrmann, R. (2002). Small nuclear ribonucleoprotein remodeling during catalytic activation of the spliceosome. Science *298*, 2205–2208.

Mishima, M., Kaitna, S., and Glotzer, M. (2002). Central spindle assembly and cytokinesis require a kinesin-like protein/RhoGAP complex with microtubule bundling activity. Dev. Cell *2*, 41–54.

Mohler, W. A., Simske, J. S., Williams-Masson, E. M., Hardin, J. D., and White, J. G. (1998). Dynamics and ultrastructure of developmental cell fusions in the *Caenorhabditis elegan*s hypodermis. Curr. Biol. *8*, 1087–1090.

Mohler, W. A., and Squirrell, J. M. (2000). Multiphoton imaging of embryonic development. In: Imaging Neurons: A Laboratory Manual, ed. R. Yuste, F. Lanni, and A. Konnerth, Cold Spring Harbor, NY: Cold Spring Harbor Laboratory Press, 21.21–21.11.

Nelson, K. K., and Lemmon, S. K. (1993). Suppressors of clathrin deficiency: overexpression of ubiquitin rescues lethal strains of clathrin-deficient *Saccharomyces cerevisiae.* Mol. Cell Biol. *13*, 521–532.

O'Connell, K. F., Leys, C. M., and White, J. G. (1998). A genetic screen for temperature-sensitive cell-division mutants *of Caenorhabditis elegans.* Genetics *149*, 1303–1321.

Oeffinger, M., and Tollervey, D. (2003). Yeast Nop15p is an RNA-binding protein required for pre-rRNA processing and cytokinesis. EMBO J. *22*, 6573–6583.

Orci, L., Tagaya, M., Amherdt, M., Perrelet, A., Donaldson, J. G., Lippincott-Schwartz, J., Klausner, R. D., and Rothman, J. E. (1991). Brefeldin A, a drug that blocks secretion, prevents the assembly of non-clathrin-coated buds on Golgi cisternae. Cell *64*, 1183–1195.

Parry, H., McDougall, A., and Whitaker, M. (2005). Microdomains bounded by endoplasmic reticulum segregate cell cycle calcium transients in syncytial *Drosophila* embryos. J. Cell Biol. *171*, 47–59.

Pitt, J. N., Schisa, J. A., and Priess, J. R. (2000). P granules in the germ cells of *Caenorhabditis elegans* adults are associated with clusters of nuclear pores and contain RNA. Dev. Biol. *219*, 315–333.

Poteryaev, D., Squirrell, J. M., Campbell, J. M., White, J. G., and Spang, A. (2005). Involvement of the actin cytoskeleton and homotypic fusion in ER dynamics in *C. elegans.* Mol. Biol. Cell *16*, 2139–2153.

Powers, J., Bossinger, O., Rose, D., Strome, S., and Saxton, W. (1998). A nematode kinesin required for cleavage furrow advancement. Curr. Biol. *8*, 1133–1136.

Praitis, V., Casey, E., Collar, D., and Austin, J. (2001). Creation of low-copy integrated transgenic lines in *Caenorhabditis elegans.* Genetics *157*, 1217–1226.

Putney, J. W., Jr., and Ribeiro, C. M. (2000). Signaling pathways between the plasma membrane and endoplasmic reticulum calcium stores. Cell Mol. Life Sci. *57*, 1272–1286.

Raich, W. B., Moran, A. N., Rothman, J. H., and Hardin, J. (1998). Cytokinesis and midzone microtubule organization in *Caenorhabditis elegans* require the kinesin-like protein ZEN-4. Mol. Biol. Cell *9*, 2037–2049.

Salmon, E. D., and Segall, R. R. (1980). Calcium-labile mitotic spindles isolated from sea urchin eggs (*Lytechinus variegatus*). J. Cell Biol. *86*, 355–365.

Schisa, J. A., Pitt, J. N., and Priess, J. R. (2001). Analysis of RNA associated with P granules in germ cells of *C. elegans* adults. Development *128*, 1287–1298.

Severson, A. F., Hamill, D. R., Carter, J. C., Schumacher, J., and Bowerman, B. (2000). The aurora-related kinase AIR-2 recruits ZEN-4/CeMKLP1 to the mitotic spindle at metaphase and is required for cytokinesis. Curr. Biol. *10*, 1162–1171.

Seydoux, G. (1996). Mechanisms of translational control in early development. Curr. Opin. Genet. Dev. *6*, 555–561.

Sheth, U., and Parker, R. (2003). Decapping and decay of messenger RNA occur in cytoplasmic processing bodies. Science *300*, 805–808.

Skop, A. R., Bergmann, D., Mohler, W. A., and White, J. G. (2001). Completion of cytokinesis in *C. elegans* requires a brefeldin A-sensitive membrane accumulation at the cleavage furrow apex. Curr. Biol. *11*, 735–746.

Skop, A. R., Liu, H., Yates, J., 3rd, Meyer, B., J., and Heald, R. (2004). Dissection of the mammalian midbody proteome reveals conserved cytokinesis mechanisms. Science *305*, 61–66.

Strome, S., and Wood, W. B. (1983). Generation of asymmetry and segregation of germ-line granules in early *C. elegans* embryos. Cell *35*, 15–25.

Sulston, J., and Hodgkin, J. (1988). Methods. In: The Nematode *Caenorhabditis elegans*, ed. W. B. Wood, Plainview, NY: Cold Spring Harbor Laboratory Press, 587–606.

Thomas, C., DeVries, P., Hardin, J., and White, J. (1996). Four-dimensional imaging: computer visualization of 3D movements in living specimens. Science *273*, 603–607.

Timmons, L., Court, D. L., and Fire, A. (2001). Ingestion of bacterially expressed dsRNAs can produce specific and potent genetic interference in *Caenorhabditis elegans.* Gene *263*, 103–112.

van Dijk, E., Cougot, N., Meyer, S., Babajko, S., Wahle, E., and Seraphin, B. (2002). Human Dcp *2*, a catalytically active mRNA decapping enzyme located in specific cytoplasmic structures. EMBO J. *21*, 6915–6924.

Verbrugghe, K. J., and White, J. G. (2004). SPD-1 is required for the formation of the spindle midzone but is not essential for the completion of cytokinesis in *C. elegans* embryos. Curr. Biol. *14*, 1755–1760.

Vlassov, A., Khvorova, A., and Yarus, M. (2001). Binding and disruption of phospholipid bilayers by supramolecular RNA complexes. Proc. Natl. Acad. Sci. USA *98*, 7706–7711.

Wang, H., Spang, A., Sullivan, M. A., Hryhorenko, J., and Hagen, F. K. (2005). The terminal phase of cytokinesis in the *Caenorhabditis elegans* early embryo requires protein glycosylation. Mol. Biol. Cell *16*, 4202–4213.

Wang, S., and Kimble, J. (2001). The TRA-1 transcription factor binds TRA-2 to regulate sexual fates in *Caenorhabditis elegans.* EMBO J. *20*, 1363–1372.

White, J. G., Squirrell, J. M., and Eliceiri, K. W. (2001). Applying multiphoton imaging to the study of membrane dynamics in living cells. Traffic *2*, 775–780.

Wilhelm, J. E., Buszczak, M., and Sayles, S. (2005). Efficient protein trafficking requires *trailer hitch*, a component of a novel ribonucleoprotein complex localized to the ER in *Drosophila.* Dev. Cell *9*, 675–685.

Wokosin, D., Squirrell, J. M., Eliceiri, K. W., and White, J. G. (2003). Optical workstation with concurrent, independent multiphoton imaging and experimental laser microbeam capabilities. Rev. Sci. Inst. *74*, 1–9.

Zipperlen, P., Fraser, A. G., Kamath, R. S., Martinez-Campos, M., and Ahringer, J. (2001). Roles for 147 embryonic lethal genes on *C. elegans* chromosome I identified by RNA interference and video microscopy. EMBO J. *20*, 3984–3992.